Chemosphere 299 (2022) 134443

Contents lists available at ScienceDirect

Chemosphere

journal homepage: www.elsevier.com/locate/chemosphere

Optimization of nitrogen feeding strategies for improving polyhydroxybutyrate production from biogas by *Methylocystis parvus* str. OBBP in a stirred tank reactor

Yadira Rodríguez [a,b], Silvia García [a,b], Rebeca Pérez [a,b], Raquel Lebrero [a,b], Raúl Muñoz [a,b,*]

[a] Department of Chemical Engineering and Environmental Technology, School of Industrial Engineering, University of Valladolid, Dr. Mergelina, s/n, 47011, Valladolid, Spain
[b] Institute of Sustainable Processes, Dr. Mergelina, s/n, 47011, Valladolid, Spain

HIGHLIGHTS

- Continuous N supply under limiting conditions did not promote PHB synthesis.
- Higher PHB productivities at 50% stoichiometric N load under feast-famine cycles.
- Feast:famine ratios ≤1:2 supported process stability at >80% stoichiometric N load.
- System robustness was compromised by NO_2^- formation.

GRAPHICAL ABSTRACT

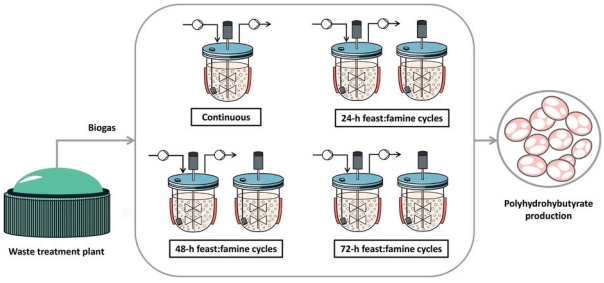

ARTICLE INFO

Handling editor: Derek Muir

Keywords:
Bioplastics
Biorefinery concept
Feeding regime
Methane oxidation
Methanotrophic bacteria
Polyhydroxyalkanoate production

ABSTRACT

The design of efficient cultivation strategies to produce bioplastics from biogas is crucial for the implementation of this biorefinery process. In this work, biogas-based polyhydroxybutyrate (PHB) production and CH_4 biodegradation performance was investigated for the first time in a stirred tank bioreactor inoculated with *Methylocystis parvus* str. OBBP. Decreasing nitrogen loading rates in continuous mode and alternating feast:famine regimes of 24 h-cycles, and alternating feast:famine regimes of 24 h:24 h and 24 h:48 h were tested. Continuous N feeding did not support an effective PHB production despite the occurrence of nitrogen limiting conditions. Feast-famine cycles of 24 h:24 h (with 50% stoichiometric nitrogen supply) supported the maximum PHB production (20 g-PHB m^{-3} d^{-1}) without compromising the CH_4-elimination capacity (25 g m^{-3} h^{-1}) of the system. Feast:famine ratios ≤1:2 entailed the deterioration of process performance at stoichiometric nitrogen inputs ≤60%.

1. Introduction

Nowadays, plastic pollution has become one of the major global environmental challenges (Heidbreder et al., 2019). The steady rise in plastic demand, which increased to 50.7 Mton by 2019 in Europe, and the global environmental problems derived from the lax plastic

* Corresponding author. Department of Chemical Engineering and Environmental Technology, School of Industrial Engineering, University of Valladolid, Dr. Mergelina, s/n, 47011, Valladolid, Spain.
E-mail addresses: yadira.rodriguez@uva.es (Y. Rodríguez), silviamaria.garcia@alumnos.uva.es (S. García), rebeca.perez@iq.uva.es (R. Pérez), raquel.lebrero@iq.uva.es (R. Lebrero), mutora@iq.uva.es (R. Muñoz).

https://doi.org/10.1016/j.chemosphere.2022.134443
Received 7 June 2021; Received in revised form 7 March 2022; Accepted 24 March 2022
Available online 29 March 2022

management policies in some countries, require an urgent reduction of our overdependence on petroleum-based plastics (Lebreton and Andrady, 2019; PlasticsEurope, 2020). Naturally synthetized polyesters constitute promising substitutes to conventional plastics (Sagong et al., 2018). These biodegradable and biocompatible thermoplastics, such as poly(3-hydroxybutyrate) (P3HB) homopolymer and its copolymer poly (3-hydroxybutyrate-co-3-hydroxyvalerate (P(3HB-*co*-3HV)), are biopolyesters that can be tuned targeting a broad range of applications (Myung et al., 2017; Steinbüchel and Valentin, 1995). For instance, PHAs have been utilized in the medical and pharmacological sectors, in the cosmetic industry or for agricultural and packaging applications (Choi et al., 2020). Today, the commercial production of polyhydroxyalkanoates (PHAs) is hampered by the high monetary costs of raw materials, which account for up to 40–50% of the total production costs (Levett et al., 2016; Pérez et al., 2020). In 2020, the PHA global production represented only 1.7% (0.3% more than in 2018) of the bioplastics market (2.1 million tonnes) (EuropeanBioplastics and novaInstitute, 2020). With PHB selling prices ranging from 5 to 6 € kg^{-1}, PHAs cannot yet compete with their petroleum-based counterparts (1.0 and 1.5 € kg^{-1} for polypropylene and polyethylene, respectively) (Khatami et al., 2021; van den Oever et al., 2017; Vandi et al., 2018).

Thus, significant efforts are being directed to find cost-effective carbon sources for PHA production (whey, molasses, crude glycerol, fatty acids, etc.) (Riedel and Brigham, 2020). Beyond its use as a renewable gas fuel, biogas has recently attracted much attention as a low-cost carbon source for the manufacturing of PHA and other value-added products based on its high content of CH_4 (50–70%) (Cantera et al., 2019; López et al., 2018; Mühlemeier et al., 2018; Muñoz et al., 2015). A recent geographical analysis demonstrated that integrating PHB production with heat and power cogeneration from biogas results in a cost-competitive production of PHA (with selling prices as low as 1.5 € kg^{-1}). Additionally, when biogas is entirely devoted to PHA production, production costs are viable (4.1 € kg^{-1}) in countries with more affordable energy prices (Pérez et al., 2020). Hence, integrated biorefineries involving alternative uses of biogas can potentially contribute to rise the biogas sector from the standstill experienced during the last three years (EBA, 2020).

PHA biosynthesis using biogas is based on the ability of type-II aerobic methane oxidizing bacteria, namely methanotrophs, to form biopolymer inclusions under growth-essential nutrient deprivation (e.g. nitrogen or phosphorous) and methane availability (Asenjo and Suk, 1986; Hanson and Hanson, 1996). Among methanotrophs, the strain *Methylocystis parvus* OBBP is regarded as a highly PHB-productive microorganism (Bordel et al., 2019b; Jiang et al., 2016; Sundstrom and Criddle, 2015). This strain was first isolated in 1970 by Whittenbury et al. (1970). Despite lacking soluble methane monoxygenase activity, *M. parvus* is a representative of type-II methanotrophs, with capability to fix nitrogen and to assimilate carbon from CH_4 through the serine pathway (del Cerro et al., 2012; Vecherskaya et al., 2009). There is a strong consensus in literature about the high PHB accumulation capacity of this strain, which can achieve PHB contents of up to 49.4% following culture media optimization (Sundstrom and Criddle, 2015) or up to 46% and 50% after ammonium and nitrate limitation, respectively (Pieja et al., 2011; Rostkowski et al., 2013). In the presence of the limiting growth factor in the culture broth, the accumulated PHB provides *M. parvus* a competitive advantage for rapid growth, with a specific growth rate of 0.154 h^{-1} (1.4 times higher than the specific growth rate on methane) (Bordel et al., 2019b; Pieja et al., 2011).

Continuous suspended-growth chemostat processes in fermenters are regarded as the optimum platform for PHA production from biogas since they enable the control of environmental conditions and nutrient feed, process operation under sterile conditions and an effective CH_4 mass transfer and biomass harvesting (AlSayed et al., 2018; Koller and Muhr, 2014; López et al., 2019). However, prior large scale implementation, methanotrophic growth under nutrient balanced conditions and PHA biosynthesis under unbalanced conditions, i.e. the two stages comprised in PHB production, need to be optimized by adapting process design to the physiological characteristics of the biological system (Kaur and Roy, 2015; Koller, 2018). A previous work evaluating the influence of sequential limitations of N-nitrate, N-nitrate + O_2 and N-nitrate + CH_4 on a mixed methanotrophic consortium reported that under all cyclical operating conditions *M. parvus* selection was favoured in the 4-L bioreactor. Particularly, in the N-limiting reactor the PHA accumulation achieved was of ~11% (w/w) after 11 cycles (Pieja et al., 2012). However, a decreasing trend in PHB content was observed throughout the implementation of these 24-h cycles, and the CH_4 biodegradation capacity of the system was not described.

Despite *M. parvus* is known for its PHB capacity under nitrogen limitation under continuous CH_4 supply, there are no previous investigations in literature addressing process optimization with the aim of supporting continuous CH_4 biodegradation under non-balanced nutrient conditions and simultaneous PHB production. This work reports for the first time a comparative analysis of different nitrogen supply strategies implemented to optimize PHB production coupled with continuous biogas utilization in a stirred tank bioreactor using the strain *Methylocystis parvus* OBBP. More specifically, the influence of (i) decreasing nitrogen loading rate (110%, 80%, 60% and 40% of the stoichiometric nitrogen requirements) under continuous mode and alternating feast:famine periods under discontinuous mode (24-h cycles), and (ii) 24 h:24 h and 24 h:48 h feast:famine cycles supplementing the stoichiometric nitrogen requirements, on PHB productivity and CH_4 biodegradation was systematically assessed.

2. Materials and methods

2.1. Culture media and chemicals

Mineral salt medium containing nitrogen in the form of potassium nitrate (hereinafter referred to as NMS), or alternatively nitrogen free mineral salt medium (NFMS), were used. Nitrogen concentration was modified depending on the nitrogen supplementation strategy of each test series. Unless otherwise stated, the NMS (pH 6.8) contained (per liter of distilled water): KNO_3, 1 g; $MgSO_4{\cdot}7H_2O$, 1.1 g; $CaCl_2{\cdot}2H_2O$, 0.2 g; $CuSO_4{\cdot}5H_2O$, 1 mg; $FeSO_4{\cdot}7H_2O$, 0.5 mg; $ZnSO_4{\cdot}7H_2O$, 0.4 mg; $Na_2MoO_4{\cdot}2H_2O$, 0.4 mg; Fe-EDTA, 0.38 mg; $Na_2EDTA{\cdot}2H_2O$, 0.3 mg; $CoCl_2$, 0.03 mg; $MnCl_2{\cdot}4H_2O$, 0.02 mg; H_3BO_3, 0.015 mg and $NiCl_2{\cdot}6H_2O$, 0.01 mg. A phosphate buffer solution containing 72 g L^{-1} $Na_2HPO_4{\cdot}12H_2O$ and 26 g L^{-1} KH_2PO_4 was added to the corresponding mineral salt medium (10 mL per liter) following autoclave sterilization at 121 °C for 21 min and subsequent cooling.

All chemicals above mentioned and reagents/solvents for PHB analysis (chloroform ≥99%, 1-propanol 99.7%, hydrochloric acid 37% w/v and benzoic acid ≥99.5% as internal standard) were purchased from PanReac AppliChem (Spain) unless otherwise specified. Potassium nitrate was obtained from COFARCAS (Spain). Poly(3-hydroxybutyrate-co-3-hydroxyvalerate) (PHBV) with a 3HB fraction of 88% was provided by Sigma-Aldrich (USA). Synthetic biogas (70/30% v/v CH_4:CO_2), oxygen (≥99.5%) and methane (≥99.995%) were supplied by Abelló Linde S.A. (Spain). Since methanotrophic growth and PHA accumulation has been already demonstrated under the presence of H_2S, this minor biogas contaminant was not included in the mixture to avoid operational problems (López et al., 2018).

2.2. Bacterial strain and inocula preparation

Cryopreserved cells of *Methylocystis parvus* strain OBBP in glycerol at −80 °C were kindly supplied by Biopolis S.L. (Valencia, Spain). The bacterium was first cultivated in NMS in an oxygen and methane atmosphere for a period of two weeks followed by pre-inoculum preparation. The pre-inoculum was prepared by transferring 5 mL of *M. parvus* culture into NMS (50 mL) contained in 125 mL serum bottles closed with butyl rubber stoppers and aluminum caps. The headspace of the serum

bottles was supplied with an oxygen and methane gas mixture at a 2:1 M ratio, which was restored on a daily basis to support methanotrophic growth by gassing pure oxygen for 5 min and replacing 25 mL with pure methane. Pre-inoculum cultures were grown at 25 °C and 250 rpm in a rotary shaker (Thermo Fisher Scientific Inc., USA) for a week. Then, five sterile gas-tight bottles (2.2 L) containing 386 mL of NMS were supplemented with 4 mL of the buffer solution and inoculated with 10 mL of *M. parvus* pre-inoculum. Chlorobutyl septa and aluminium screw caps were used to maintain gas-tightness in the 2.2 L bottles. A 100 L Tedlar® bag (Sigma-Aldrich, USA) with an O_2:CH_4 composition of 66.7:33.3% (v/v) was used to provide the desired headspace atmosphere by flushing the gas mixture with a compressor for nearly 3 min. The bottles were incubated under controlled temperature and mixing conditions (25 °C, 300 rpm) on a Variomag Multipoint 6 magnetic stirrer (Thermo Scientific, USA) for ~10 days. The headspace of the bottles was replaced with the above described gas mixture three days prior cells harvesting, which was carried out by centrifugation (10,000 rpm, 8 min) in sterile centrifuge tubes. Biomass pellets were re-suspended either into fresh NMS or NFMS (depending on the nitrogen feeding strategy) and concentrated to deliver a 250 mL-inoculum with a total solids concentration ranging from 5.4 to 6.1 g L^{-1}. All these procedures were carried out under sterile conditions.

2.3. Bioreactor set-up

All experiments were performed in a bench-top borosilicate glass Biostat®A bioreactor (Sartorius Stedim Biotech GmbH, Germany) with a working volume of 2.5 L (Fig. 1). The bioreactor enabled process control and real-time monitoring of pH, temperature and dilution rate. For that purpose, the vessel was fitted with a temperature sensor and digital pH and level probes. The bioreactor was constructed with a 2 μm-pore stainless steel gas diffuser (Supelco, USA), which was placed at the bottom of the vessel to sparge the air:biogas mixture at 42 mL min^{-1} (corresponding to 60 min of gas residence time). The gas composition resulting from the mixture of synthetic biogas and pressurized air was adjusted to a O_2:CH_4 concentration of 16%:8% *v/v* by using a mass flow controller (GFC17, Aalborg™, USA) and a rotameter for the biogas and air streams, respectively. Continuous stirring at 600 rpm was provided with a six-blade Rusthon turbine to ensure enough turbulence without cell damage, whereas a heating blanket was used to maintain the operating temperature at 30 °C. The pH of the culture broth was maintained at 7.0 by addition of 4 N NaOH.

2.4. Experimental procedure

2.4.1. Test series 1 - CH_4 biodegradation and PHB production under continuous nitrogen feeding

This test series assessed PHB accumulation under continuous NMS supply at decreasing nitrogen loading rates (NLR) below stoichiometric nitrogen requirements. The chemostat was initially inoculated with 50 mL of *M. parvus* pre-inoculum resulting in a biomass concentration of 20 mg L^{-1} and operated under batch mode with an initial concentration of 276 mg $N–NO_3^-$ L^{-1} in NMS until nitrogen depletion by day 9. Then, the bioreactor was operated for 90 days at a continuous dilution rate of 0.008 h^{-1} (below the critical dilution rate, D_{crit} = 0.017 h^{-1}) under decreasing NLR in four different stages. NLRs of 75, 54, 41 and 27 mg d^{-1} were set during stages I, II, III and IV, respectively, which corresponded to 110%, 80%, 60% and 40% of the stoichiometric nitrogen requirements based on *M. parvus* composition and yield, and the previously determined CH_4 mass transfer capacity of the bioreactor a 600 rpm. On average, each stage was run for 25 days (five times the hydraulic retention time), except for stage I that lasted 10 days.

2.4.2. Test series 2 - CH_4 biodegradation and PHB production under different feast-famine regimes (24 h cycles, discontinuous feeding)

Following autoclave sterilization of the bioreactor, *M. parvus* was inoculated at an initial biomass concentration of 540 mg L^{-1}. A higher concentration was used in Tests Series 2, 3 and 4 compared to Test Series 1 in order to reduce the time required to overcome biological limitation. The bioreactor was initially operated under batch cultivation and nitrogen deprived conditions for 72 h in order to initiate PHB synthesis. Then, the culture was subjected to a cyclic nitrogen feast-famine regime at varying feeding profiles. The operation was conducted in four different stages of seven feast-famine 24 h cycles. To this end, NMS containing a $N–NO_3^-$ concentration of 331 mg L^{-1} was supplied at feeding rates of 0.5 and 0 L d^{-1} corresponding to the growth and PHB accumulation phases, respectively. NMS feeding periods of 11, 8, 6 and 4 h were set in stages I, II, III and IV, respectively, which corresponded to the same NLRs set in Test series 1 (75, 54, 41 and 27 mg $N–NO_3^-$ per cycle) (Table 1).

2.4.3. Test series 3 - CH_4 biodegradation and PHB production under a 24 h–24 h feast-famine regime

The bioreactor was inoculated at an initial biomass concentration of 560 mg L^{-1} and operated under nitrogen limiting conditions in batch mode for 72 h. Batch cultivation was followed by 12 sequential feast-famine cycles consisting of continuous NMS feeding at 0.5 L d^{-1} for

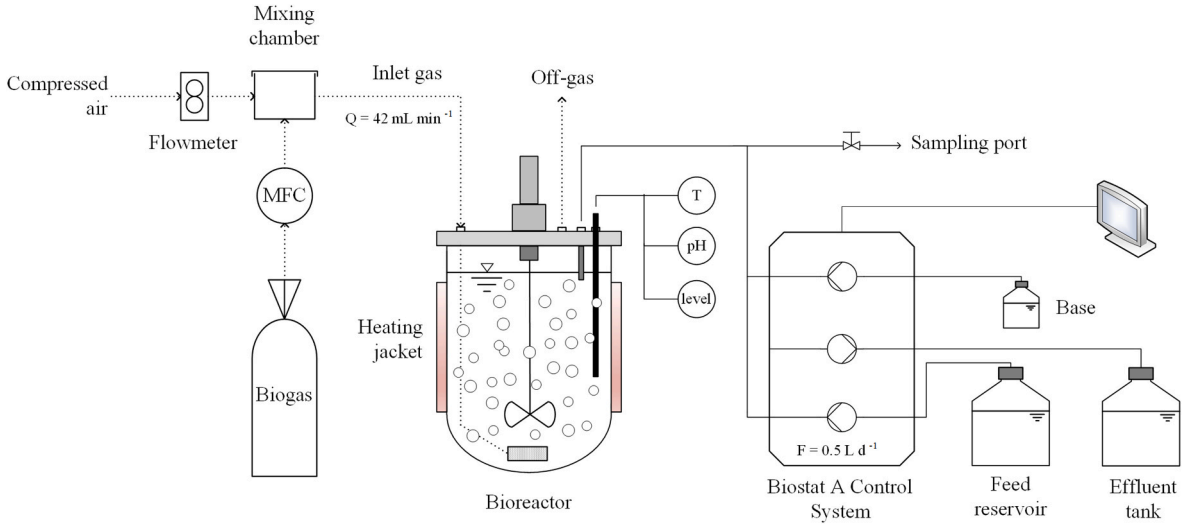

Fig. 1. Schematic representation of the experimental set-up.

Table 1
Detailed operating conditions for the different continuous and cyclic feeding strategies tested.

Test	Stage	Period (days)	Operation Mode	Feast-famine cycles (h:h)	N– NO_3^- Feed Concentration (mg L^{-1})	N– NO_3^- Loading Rate (mg $cycle^{-1}$) (mg d^{-1})*	N– NO_3^- Supply (%)
1	I	10	Continuous	–	150	75*	110
	II	25	Continuous	–	108	54*	80
	III	25	Continuous	–	82	41*	60
	IV	25	Continuous	–	54	27*	40
2	I	7	Cyclic	11:13	328	75	110
	II	7	Cyclic	8:16	328	54	80
	III	7	Cyclic	6:18	328	41	60
	IV	7	Cyclic	4:20	328	27	40
3	I	24	Cyclic	24:24	135	68	50
4	I	20	Cyclic	24:48	135	68	33

24 h followed by 24 h of discontinuous operation under nitrogen deprived conditions. The nitrogen load of each cycle was 68 mg N–NO_3^-, which corresponded to the stoichiometric N requirements. The bioreactor was operated for 24 days under feast and famine conditions (Table 1).

2.4.4. Test series 4 - CH_4 biodegradation and PHB production under a 24 h–48 h feast-famine regime

M. parvus was inoculated at an initial biomass concentration of 610 mg L^{-1}. Then, the bioreactor was batchwise operated under nitrogen limiting conditions for 72 h as described in Test series 2 and 3. Sequential feast-famine cycles of 24 h–48 h were implemented for 21 days (comprising a total of 7 cycles) via continuous NMS feeding at a flowrate of 0.5 L d^{-1} for 24 h followed by 48 h of batch incubation without mineral medium supply. The nitrogen load per cycle was set at 68 mg N–NO_3^- per cycle.

Process monitoring was conducted at the end of both the growth and accumulation phases in Tests series 2, 3 and 4, or periodically (every 2–3 days) during continuous operation in Test series 1. Gas samples were withdrawn in duplicate with a 100 μL Hamilton gas-tight syringe from the inlet and outlet gas sampling points to monitor the concentration of CH_4, O_2 and CO_2. The outlet gas flowrate and the pressure drop caused by the gas diffuser were also measured. Aliquots of 40 mL of the culture broth were withdrawn from the bioreactor for the determination of the optical density (OD), total suspended solids (TSS) concentration and pH. Culture broth (1.5 mL in duplicate) was centrifuged at 10,000 rpm for 10 min and stored at −20 °C after supernatant decanting for PHB analysis. Filtrate collected from TSS determination was used for the analysis of the total dissolved nitrogen (TN), total organic carbon (TOC), NO_2^- and NO_3^- concentrations.

2.5. Analytical procedures

Microbial PHB was quantified in an Agilent 7820A gas chromatograph (GC) coupled to an Agilent 5977E mass spectrometer (MS) (Agilent Technologies, USA) following hydrochloric acid propanolysis (Rodríguez et al., 2020a). Gas chromatographic conditions are detailed elsewhere (Chen et al., 2020). Biomass concentration was determined as grams of TSS per liter of cell culture according to Standard Methods (2540 Solids, APHA, 2018) using Merck MF Millipore (0.45 μm pore size) membrane filters (Merck, Germany). A SPECTROstar Nano (BMG LABTECH, Germany) spectrophotometer was used to monitor bacterial growth at 600 nm pH measurements were carried out with a Basic 20 pH meter (Crison, Spain). The quantification of nitrite and nitrate concentrations was performed by ion-exchange liquid chromatography (IC) with conductivity detection (Waters 432, Waters Corporation, USA). TOC and TN measurements in filtered samples were performed simultaneously in a TOC-$L_{CSH/CSN}$ analyser coupled with a TNM-1 unit (Shimadzu, Japan). The inlet and outlet gas composition (CH_4, CO_2 and O_2) was analyzed in a Bruker 430 gas chromatograph (GC) coupled with a thermal conductivity detector (TCD) (Bruker Corporation, USA). The GC-TCD was equipped with CP-Molsieve 5A and CP-PoraBOND Q columns. Pressure drops were recorded using a PN7097 electronic pressure sensor (Ifm Electronic, Germany). Finally, the outlet gas flowrate was determined using the water displacement method.

2.6. Data treatment

The methane elimination capacity (CH_4-EC), the methane removal efficiency (CH_4-RE) and the volumetric production of CO_2 (PCO_2) were used as the main performance indicators of the bioreactor and calculated as described elsewhere (Rodríguez et al., 2020b). All results are presented as average values with standard deviations of duplicates analyses, except for TN and anions. Statistical analysis was performed using one-way ANOVA with a significance $P \leq 0.05$. Software OriginPro 8.5.0 SR1 (OriginLab Corp.) was used for data treatment and graphics preparation.

3. Results

3.1. Test series 1 - CH_4 biodegradation and PHB production under continuous nitrogen feeding

Under batch cultivation, *M. parvus* supported a maximum N–NO_3^- consumption rate of 64.0 mg L^{-1} d^{-1} ($R^2 = 0.997$) (from day 5 to day 8) and a complete N–NO_3^- removal by day 9 (Fig. 2a). During this initial stage, an almost negligible denitrification activity was observed, with N–NO_2^- concentrations ranging from 0.6 to 1.1 mg L^{-1}. From day 9 onwards, the bioreactor was operated under steady decreasing nitrogen loading rates. Neither the presence of nitrate nor nitrite in the culture broth was recorded regardless of the operating stages, whereas a residual total nitrogen content of 6.1 ± 1.7 mg L^{-1} was always observed. The pH of the cultivation broth remained constant at 7.05 ± 0.26 along the different stages. The maximum biomass concentration recorded at the end of the batch phase (1.43 ± 0.04 g L^{-1}, day 9) levelled off and remained at 1.35 ± 0.06 g L^{-1} in stage I (Fig. 2b). The reduction of the nitrogen load from 75 to 54 mg d^{-1} (stage II) resulted in a sharp drop in the biomass concentration within the first seven days of stage II, which finally stabilized at 0.86 ± 0.04 g L^{-1}. In the following operating stages (stages III and IV), the biomass concentrations averaged 0.91 ± 0.07 g L^{-1} and 1.06 ± 0.13 g L^{-1}, respectively. On the other hand, process operation under nitrogen sufficient conditions in stage I resulted in PHB contents of 1.0 ± 0.6%, while N feeding below the stoichiometric requirements resulted in PHB contents of 2.1 ± 2.2, 1.8 ± 1.3 and 2.2 ± 1.0% (corresponding to PHB productivities of 4, 3 and 5 g-PHB m^{-3} d^{-1}) in stages II, III and IV, respectively.

A maximum CH_4-EC of 47.9 ± 0.5 g m^{-3} h^{-1} was reached at the end of the initial batch period (day 7) followed by a decrease and stabilization at 26.4 ± 0.5 g m^{-3} h^{-1} (corresponding to a CH_4-RE of 47 ± 1%) when continuous operation was initiated (stage I) (Fig. 2c). The EC remained similar in the subsequent operating stages, with CH_4-ECs of 25.5 ± 2.3, 25.2 ± 2.1 and 24.2 ± 2.9 g m^{-3} h^{-1} (corresponding to

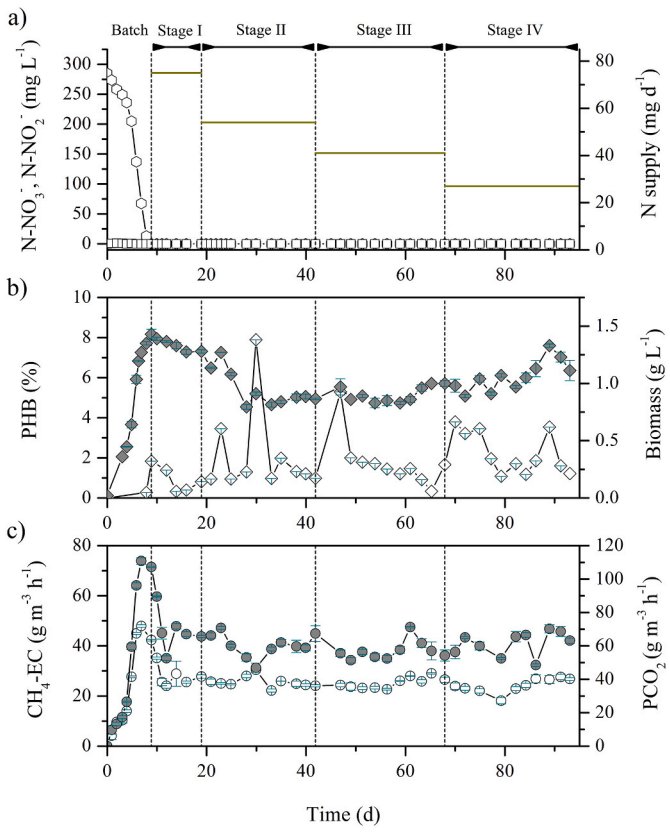

Fig. 2. Time course of **(a)** NO_3–N (hexagons) and NO_2–N (squares), N supply (continuous line) **(b)** PHB content (empty diamonds) and biomass concentration (solid diamonds), and **(c)** CH_4-EC (empty circles) and PCO_2 (solid circles) in Test series 1. Vertical dashed lines separate the different operating stages.

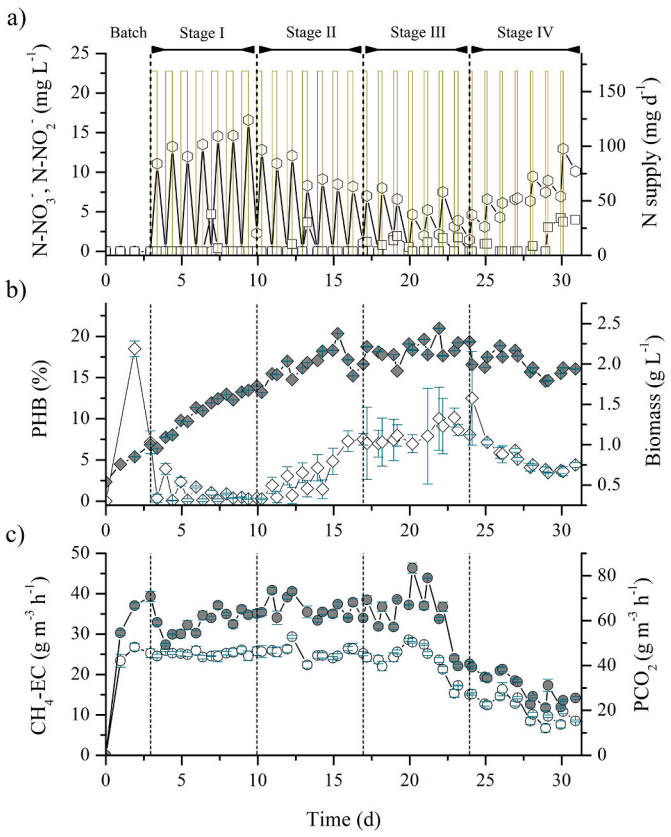

Fig. 3. Time course of **(a)** NO_3–N (hexagons) and NO_2–N (squares), N supply (continuous line) **(b)** PHB content (empty diamonds) and biomass concentration (solid diamonds), and **(c)** CH_4-EC (empty circles) and PCO_2 (solid circles) in Test series 2. Vertical dashed lines separate the different operating stages.

methane removal efficiencies of 43.5 ± 2.3, 43.2 ± 3.4 and 43.5 ± 4.2%) recorded in stages II, III and IV, respectively. Similarly, the bioreactor achieved a maximum PCO_2 of 110.8 ± 2.0 g m^{-3} h^{-1} by day 7 at the end of the exponential growth phase. Then, PCO_2 dropped sharply during the first two days stabilizing at 64.9 ± 7.2, 60.3 ± 7.0, 57.1 ± 5.8 and 61.7 ± 7.2 g m^{-3} h^{-1} in stages I, II, III and IV, respectively. Along with the reduction of the nitrogen load throughout the different stages, no statistically differences were observed in the methane mineralization ratio (PCO_2/CH_4-EC), which averaged 2.5 ± 0.2, 2.4 ± 0.4, 2.3 ± 0.2 and 2.6 ± 0.3 g CO_2 (g CH_4)$^{-1}$ during stages I, II, III and IV, respectively. Likewise, the consumed O_2 to CH_4 ratio remained constant at 1.58 ± 0.09 throughout the entire experiment.

3.2. Test series 2 – CH_4 biodegradation and PHB production under different feast-famine regimes (24-h cycles, discontinuous feeding)

At the end of the feeding periods, N–NO_3^- concentrations of 13.7 ± 1.8, 10.0 ± 1.9, 6.1 ± 1.5 and 7.9 ± 2.8 mg L^{-1} were observed in stages I, II, III and IV, respectively (Fig. 3a). By the end of the limitation periods, complete removal of N–NO_3^- was achieved in stages I and II, with partial elimination (~60%) in stage III. From cycle 18 (stage III) onwards, the N–NO_3^- concentration in the cultivation broth at the end of the cycles gradually increased, reaching a concentration of 10.1 mg L^{-1} by the end of the experiment (stage IV). Low concentrations of N–NO_2^- (≤4.5 mg L^{-1}) were observed throughout the test. However, from cycle 27 onwards (stage IV) N–NO_2^- remained in the system with a concentration of 3.8 ± 0.5 mg L^{-1} (Fig. 3a). In addition, the presence of residual total nitrogen increased from 8.1 ± 6.0 (stage I) to 63.0 ± 12.8 mg L^{-1} (stage IV). Cultivation broth pH of 6.9 ± 0.1, 7.0 ± 0.1, 7.1 ± 0.0 and 7.2 ± 0.0 were recorded in stages I, II, III and IV, respectively. Following inoculation, biomass concentration steadily increased throughout the cycles until the end of stage II, where a maximum concentration of 2.38 ± 0.01 g L^{-1} was reached. Afterwards, biomass concentration levelled off at 2.19 ± 0.12 g L^{-1} during stage III, whereas cell concentration in stage IV dropped to values below 1.90 ± 0.04 g L^{-1} from cycle 25 onwards (Fig. 3b). Batch cultivation under N deprivation and presence of methane resulted in an initial PHB content of 7.1 ± 1.4% in stage I, which gradually decreased to 0.4 ± 0.0% by the end of stage I with the implementation of the cyclic operation. *M. parvus* exhibited a greater PHB accumulation during stage II, where PHB content varied from 1.9 ± 0.9% (cycle 8) to 7.5 ± 0.7% (cycle 14), corresponding to a volumetric PHB productivity of 12 g-PHB m^{-3} d^{-1} at the end of the stage. During these two first stages, both PHB consumption and accumulation phases in each cycle were clearly differentiated regarding PHB content, as shown in Fig. 3b. In stage III, the PHB content remained stable at 8.0 ± 1.0%, corresponding to a volumetric PHB productivity of 9 g-PHB m^{-3} d^{-1}. Finally, PHB content in cells during stage IV dropped below 4.5% from cycle 25 onwards.

Following batch cultivation (day 3), the system exhibited a CH_4-EC and a PCO_2 of 25.3 ± 1.1 and 70.8 ± 2.3 g m^{-3} h^{-1}, respectively (Fig. 3c). Subsequently, CH_4-EC averaged 25.3 ± 1.4 g m^{-3} h^{-1} (corresponding to removal efficiencies of 42.9 ± 2.1%) in stages I and II, and during the first four cycles of stage III (cycles 15–18). From cycle 19 (stage III) to cycle 25 (stage IV), a sharp decrease in CH_4-EC was observed, which eventually stabilized at 8.8 ± 1.4 g m^{-3} h^{-1}. Similarly, PCO_2 did not vary significantly among stages I, II and III with values of 59.4 ± 5, 65.4 ± 4.6 and 61.9 ± 13.2 g m^{-3} h^{-1}, respectively, while a gradual decrease to stable values of 24.7 ± 3.4 g m^{-3} h^{-1} was recorded in stage IV. The reduction in the nitrogen loading rates induced a slight increase in PCO_2/CH_4-EC from 2.4 ± 0.2 g CO_2 g^{-1} CH_4 (stage I) to 2.7

± 0.3 g CO_2 g^{-1} CH_4 in stages III and IV. Likewise, the consumed O_2 to CH_4 ratio in stage I (1.48 ± 0.08) significantly differed from those values observed in the subsequent stages (1.55 ± 0.05, 1.63 ± 0.10 and 1.69 ± 0.12 in stages II, III and IV, respectively).

3.3. Test series 3 - CH_4 biodegradation and PHB production under a 24 h–24 h feast-famine regime

After the initial cultivation period under N limiting conditions, the culture was subjected to a 24 h:24 h cyclic operation (Fig. 4a). The bioreactor supported a complete removal of nitrogen in the form of nitrate from the first cycle until the end of the test, with no formation of nitrite observed. On the other hand, a residual nitrogen concentration in the culture broth of 7.9 ± 3.2 mg L^{-1} was observed, while the pH remained stable at 6.82 ± 0.10 during the entire experiment. Following inoculation, the biomass concentration increased up to 1.33 ± 0.01 g L^{-1} by the end of batch cultivation. Biomass concentration in the culture broth progressively increased alternating decreases and increases after each feast and famine phase, respectively, reaching a final concentration of 2.55 ± 0.01 g L^{-1} by the end of the cycles. The PHB content, which accounted for 34.3 ± 2.4% at the end of the batch cultivation, steadily decreased to 1.8 ± 0.2% by cycle 7 with the implementation of the feast-famine regime. However, from the famine phase of cycle 7 onwards (day 16), the PHB content in *M. parvus* exhibited a gradual increase to finally stabilize during the last two cycles at average PHB contents ranging from 13.7 ± 1.5 to 21.6 ± 2.8% in the feast and famine phases, respectively (which represented a PHB productivity of 20 g-PHB m^{-3} d^{-1}).

During batch cultivation, the system supported an initial CH_4-EC of 23.3 ± 1.0 g m^{-3} h^{-1}, which decreased to 9.0 ± 2.0 g m^{-3} h^{-1} by day 3 of operation. CH_4-ECs fluctuated from ~11 to ~23 g m^{-3} h^{-1} during cycle 1, while from cycle 2 onwards CH_4-ECs remained stable at 24.9 ± 1.5 g m^{-3} h^{-1} (Fig. 4c) (corresponding to CH_4-REs of 44 ± 2%). Similarly, PCO_2 fluctuated between ~24 and ~59 g m^{-3} h^{-1} at the beginning of the cyclic operation, and rapidly stabilized at 64.5 ± 3.8 g m^{-3} h^{-1}. Moreover, no significant differences were observed neither in CH_4-ECs (24.5 ± 1.5 and 25.2 ± 1.6 g m^{-3} h^{-1}) nor in PCO_2 (64.5 ± 4.3 and 64.1 ± 3.6 g m^{-3} h^{-1}) at the corresponding feast and famine phases during the steady state. These values resulted in an average mineralization ratio of 2.6 ± 0.2 g CO_2 g^{-1} CH_4 and in a consumed O_2 to CH_4 ratio of 1.60 ± 0.07.

3.4. Test series 4 - CH_4 biodegradation and PHB production under a 24 h–48 h feast-famine regime

Following batch operation, nitrate was completely consumed only within the first two feast-famine cycles. From cycle 3 onwards, accumulations of nitrate (up to ~38 mg L^{-1} $N\text{–}NO_3^-$ by day 22) and, to a lesser extent of nitrite (1.6 ± 0.6 mg L^{-1} $N\text{–}NO_2^-$), were observed (Fig. 5a). Furthermore, a residual nitrogen content in the culture broth of 4.3 ± 2.0 mg L^{-1} was recorded. The pH of the cultivation broth averaged 7.0 ± 0.6, regardless of the feast and famine phases. Initially, a biomass concentration of 0.91 ± 0.00 g L^{-1} was reached during batch cultivation, which steadily increased (despite marked fluctuations) up to 1.26 ± 0.0 g L^{-1} by the end of cycle 3 (Fig. 5b). From cycle 4 onwards, biomass concentration gradually decreased leading to a final concentration of 0.89 ± 0.0 g L^{-1}. Similarly, PHB accumulation, which accounted for 41.7 ± 3.4% at the beginning of the feast-famine operation, ranged from 27.2 ± 2% to 35.5 ± 1% within the first three cycles. These figures corresponded to a PHB productivity of 21 g-PHB m^{-3} d^{-1}. PHB content steadily decreased afterwards from 35.0 ± 0.3% to 26.1 ±

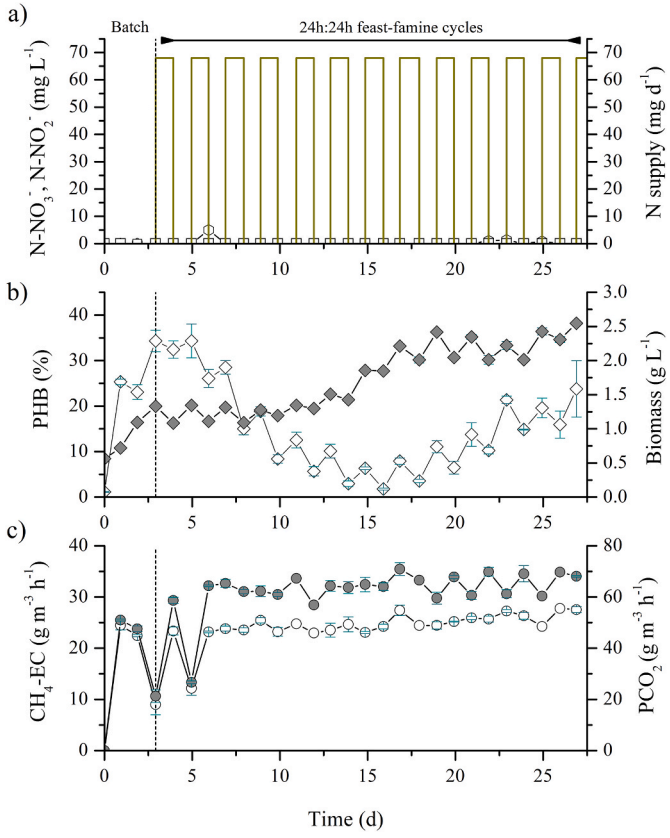

Fig. 4. Time course of **(a)** NO_3–N (hexagons) and NO_2–N (squares), N supply (continuous line) **(b)** PHB content (empty diamonds) and biomass concentration (solid diamonds), and **(c)** CH_4-EC (empty circles) and PCO_2 (solid circles) in Test series 3. Vertical dashed line separates batch from continuous operation.

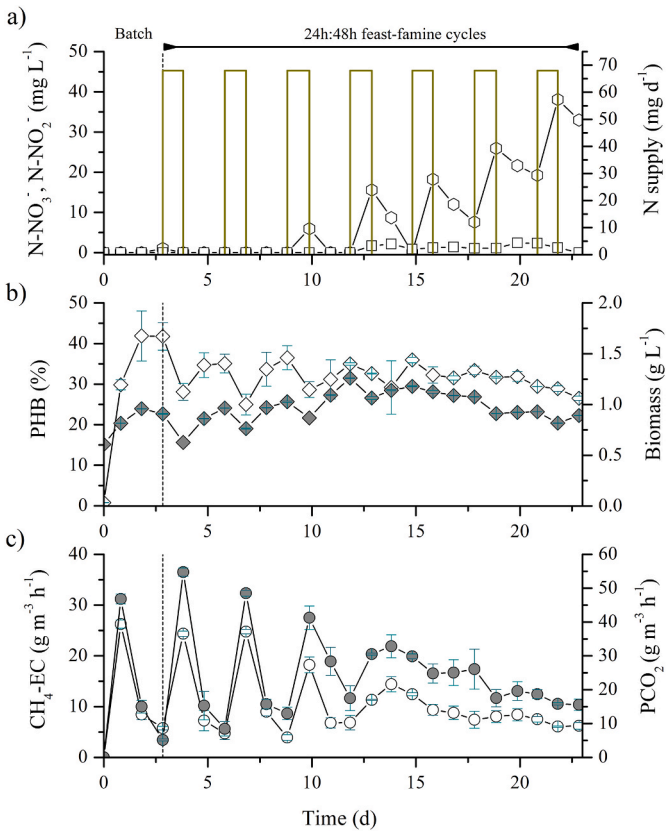

Fig. 5. Time course of **(a)** NO_3–N (hexagons) and NO_2–N (squares), N supply (continuous line) **(b)** PHB content (empty diamonds) and biomass concentration (solid diamonds), and **(c)** CH_4-EC (empty circles) and PCO_2 (solid circles) in Test series 4. Vertical dashed line separates batch from cyclic operation.

0.5% by the end of the experiment.

Following inoculation, the system reached a CH_4-EC of 26.3 ± 0.8 g m^{-3} h^{-1} by day 1, which dropped to 5.6 ± 0.3 g m^{-3} h^{-1} in the following two days. With the implementation of the 24 h:48 h feast-famine regime, CH_4-EC markedly fluctuated from 4.8 ± 0.6 to 24.6 ± 0.3 g m^{-3} h^{-1} during the first two cycles (corresponding to REs of 8 ± 1 and 40 ± 1%, respectively). Less sharp fluctuations were observed during cycles 3 and 4, stabilizing from cycle 5 onwards at 7.7 ± 1.2 g m^{-3} h^{-1} (corresponding to a CH_4-RE of 12.5 ± 2.0%) (Fig. 5c). Likewise, PCO_2 fluctuated between ~9 and ~52 g m^{-3} h^{-1} in the first two cycles. From cycle 3 onwards, PCO_2 decreased from 41.3 ± 3.5 g m^{-3} h^{-1} by day 9–15.6 ± 1.7 g m^{-3} h^{-1} at the end of the experimentation period. Throughout the feast-famine regime the mineralization ratio averaged 2.5 ± 0.6 g CO_2 (g CH_4)$^{-1}$, with values >3 g CO_2 (g CH_4)$^{-1}$ being occasionally recorded at the end of the cycle. Finally, the consumed O_2 to CH_4 ratio was 1.60 ± 0.2 regardless of the operational phase.

4. Discussion

The operational criteria for a cost-effective PHB production in a single-stage process should not only rely on the biopolymer content accumulated in the cells, but also provide favourable environmental conditions for a sustained methanotrophic activity in the long term operation. In this context, only process operation with a continuous nitrogen supply (Test Series 1) and 24 h:24 h feast:famine cycles (Test Series 3) supported a steady methane abatement (~25 g m^{-3} h^{-1}) and a complete nitrate removal. The methane elimination capacities here recorded were comparable with those reported in other STRs using methanotrophic consortia, which ranged from 20 ± 3 to 33 ± 1 g m^{-3} h^{-1} at 500 and 800 rpm, respectively (Rocha-Rios et al., 2010), although lower than those reported by Muñoz et al. (2018) at a similar stirring velocity (42.5 ± 5.4 g m^{-3} h^{-1}). Despite gas bubble disruption caused by the mechanical agitation (herein supported by a Rushton turbine) typically increases biocatalytic activity by enhancing CH_4 bioavailability in the cultivation broth, preliminary works in our lab (data not shown) suggested that high stirring rates (>600 rpm) negatively impacted CH_4-ECs likely due to the high shear stress on *M. parvus* cell membrane. Superior CH_4-ECs (~41 g m^{-3} h^{-1}) were obtained by *Methylocystis hirsuta* in a bubble column bioreactor under cyclic operation (24 h:24 h) fed with air:biogas mixtures and operated with internal gas recirculation at the same gas residence time (60 min) and a gas recirculation ratio of 30 (Rodríguez et al., 2020b). Nitrate was not found to be inhibitory per se for *M. parvus* at any of the N concentrations of the present work, which remained always below the concentration found to hinder methanotrophic activity (280 mg L^{-1} N–NO_3^-) in other type II-methanotroph such as *Methylosinus* sp. (R-45379) (Hoefman et al., 2014). Cell biosynthesis under continuous nitrogen supply (Test Series 1) and 24 h:24 h feast:famine cycles (Test Series 3) evidenced assimilative N-nitrate uptake, as only small transient peaks of nitrite were detected. This assimilatory pathway involves nitrate reduction to nitrite and further to ammonia, which are mediated by nitrate and nitrite reductases, respectively (Cai et al., 2016), and N assimilation via the glutamate cycle, a general characteristic of the *Alphaproteobacteria* class (Trotsenko and Murrell, 2008).

During Test Series 2, nitrogen feast-famine cycles of 11 h:13 h (110% N supply – stage I) and 8 h:16 h (80% N supply – stage II) supported comparable results in terms of bioreactor performance, with a stable methane biodegradation (~25 g m^{-3} h^{-1}) and total nitrogen uptake. However, under more severe nitrogen limiting conditions such as those applied in stages III and IV in Test Series 2 with a feast-famine cyclic operation of 6 h:18 h (60% N supply) and 4 h:20 h (40% N supply), respectively, and in Test Series 4 with a cyclic nitrogen deprivation phase of 48 h (33% N supply), nitrate levels in the culture broth increased with a concomitant accumulation of nitrite and a gradual deterioration of the CH_4-EC (accounting for a 65 and 69% CH_4-EC reduction in Test Series 2 and 4, respectively, by the end of the experiment). A recent paper, reporting the Genome Scale Metabolic Model of *M. parvus* OBBP, elucidated that nitrite can be produced not only via assimilatory and dissimilatory nitrate reduction during CH_4 degradation (Hoefman et al., 2014), but also via internal PHB consumption coupled to denitrification under anoxic conditions (Bordel et al., 2019b). This suggests a tentative explanation for nitrite formation in Test Series 2 (stage IV) and 4 (with N–NO_2^- concentrations of 3.8 ± 0.5 mg L^{-1} and 1.6 ± 0.6 mg L^{-1}, respectively), where the stored PHB could have been likely used as an energy source under oxygen limiting conditions. Indeed, the 2:1 O_2:CH_4 ratio present in the inlet gas stream was likely not sufficient to cope with the additional oxygen demand for PHB oxidation. *M. parvus* inability to assimilate nitrite and the concomitant deterioration of the methanotrophic activity observed under these nitrogen limiting conditions could be tentatively explained by the fact that nitrite inhibits the enzyme formate dehydrogenase (King and Schnell, 1994). This inhibition limits the generation of the reducing power required to reduce nitrite into ammonia (3 mol of NADH per 1 mol NO_2^-) via the NADH-dependent nitrite reductases. Even though the inhibitory effects of nitrite on methanotrophs are widely known (King and Schnell, 1994; Nyerges and Stein, 2009), genome sequences of closely related species, such as *Methylocystis* sp. SC2 and *Methylocystis hirsuta*, revealed the potential to cope with its toxicity through partial and complete denitrification pathways, respectively (Bordel et al., 2019a). In this sense, while nitrite concentrations above 25 mM seem to completely inhibit *M. hirsuta* growth (Nyerges et al., 2010, Rodríguez et al., 2020a, b), a certain tolerance has been observed to lower nitrite concentrations (~2 mM, Nyerges and Stein, 2009). Although nitrous oxide was not analyzed in this study, the results herein obtained did not support an active detoxification mechanism by *M. parvus*.

The CH_4 mineralization ratios under all nitrogen supply strategies investigated (2.3 ± 0.2–2.7 ± 0.3 g CO_2 (g CH_4)$^{-1}$) remained above those reported under balanced growth conditions (<2.2 g CO_2 (g CH_4)$^{-1}$) (García-Pérez et al., 2018; Rodríguez et al., 2020b) at a similar gas residence time in the bioreactor. This discrepancy may be attributed to the co-utilization of the stored PHB and CH_4 to aid NADH regeneration (4 CO_2 per $C_4H_6O_2$), particularly noticeable under severe nitrogen stress conditions (≤40% N supply) (Pieja et al., 2011; Sipkema et al., 2000). For instance, PHB content decreased by nearly 45% during the operating stage under feast-famine cycles of 4 h:18 h (stage IV - Test Series 2). However, it is also worth noting that mineralization ratios peaked occasionally above 2.8 g CO_2 (g CH_4)$^{-1}$ (corresponding to mineralization ratios above 100%), suggesting also an active endogenous cell respiration (García-Pérez et al., 2018), very likely in scenarios with longer N deprived conditions (24 h:48 h cycles - Test Series 4), where PHB exhibited only a decrease by 25% at lower ECs. Overall, the observed O_2:CH_4 consumption ratios (~1.6) were remarkably consistent with those reported by Chen et al. (2020), Karthikeyan et al. (2015) and Pieja et al. (2011) for PHB production, who estimated ratios of 1.6 (mechanistic model), 1.5 (stoichiometry) and 1.5 (empirical for *M. parvus*), respectively. Nevertheless, an increasing trend was observed under progressive nitrogen limiting conditions in Test Series 2 (e.g.: from 1.48 ± 0.08 (stage I) to 1.69 ± 0.12 (stage IV)), which could be likely attributed to the occurrence of other O_2-consuming processes such as the co-consumption of PHB (which decreased from 12.5 to 3.6% (w/w)) and dissolved organic matter associated to excreted metabolites, cell lysis or other type of contamination. In this regard, an increase in the TOC concentration from 16.8 mg L^{-1} in stage I to 368.7 mg L^{-1} in stage IV was recorded.

Nitrogen starvation for 72 h under batch operation initially yielded PHB contents ranging from 7 to 42%, which were consistent with those reported for *M. parvus* OBBP (14–50%) under nitrate limitation in serum bottles (Pieja et al., 2011; Rostkowski et al., 2013). The continuous cultivation of *M. parvus* (Test Series 1) at decreasing nitrogen loads yielded low P(3HB) accumulations (~2%) with no significant differences among stages. Interestingly, stepwise reductions in the nitrogen loading rate did not progressively boost PHB accumulation in the

cultivation broth (as moderate intracellular PHB contents were only sporadically observed). Nonetheless, *M. parvus* was able to thrive on the CO_2+CH_4 mixture regardless of the nitrogen loading rate as demonstrated by a steady elimination capacity and a constant biomass productivity. These results suggest that process operation under continuous nitrogen supply below stoichiometric requirements enabled concomitant biopolymer synthesis and consumption, as PHB may serve as a reducing power source to cover the great energy demand of MMO, allowing pMMO activity in the presence of an exogenous carbon source (i.e. CH_4) and N-nitrate assimilation (Pieja et al., 2011). In addition, this study suggested that *M. parvus* was capable of utilizing gas N_2 as nitrogen source concomitantly with NO_3^- assimilation. Indeed, biomass yields of 0.41 ± 0.05, 0.31 ± 0.06, 0.30 ± 0.02 and 0.37 ± 0.05 g biomass (g $CH_{4\ degraded}$)$^{-1}$ were recorded under N–NO_3^- loading rates representing 110, 80, 60 and 40% of the theoretical nitrogen demand at the empirical CH_4-EC. In fact, N_2 fixation in type II methanotrophs was demonstrated to occur at oxygen partial pressures of up to 0.2 atm (Murrell and Dalton, 1983; Rostkowski et al., 2013). At this point, it should be stressed that continuous PHB production systems are still quite unexplored in comparison with batch and fed-batch PHB production systems (Blunt et al., 2018; Koller, 2018).

Nevertheless, the volumetric PHB productivities herein recorded (3–5 g-PHB m^{-3} d^{-1}) were below those reported by other PHB-accumulating bacteria under continuous culture. For instance, Ramsay et al. (1990) reported a productivity of 7.2 kg-PHBV m^{-3} d^{-1} using sucrose and propionic acid as a carbon source by *Azohydromonas lata* in a single-stage CSTR. In addition to the limited bioavailability of the carbon source in the liquid phase for methanotrophs, a possible explanation to this discrepancy is that, unlike other PHB-producing microorganism, PHB synthesis by *M. parvus* is not growth-associated (Bordel et al., 2019b; Rostkowski et al., 2013). Conversely, identical N loading rates to Test Series 1 with chronological separation of both growth and accumulation phases (24 h-cycles in Test Series 2) featured different outcomes in terms of PHB accumulation. Thus, PHB consumption prevailed over PHB accumulation under an 110% N supply (11 h:13 h cycles - stage I) whereas cycles providing a larger N limitation (i.e. 8 h:16 h cycles – stage I and 6 h:18 h cycles – stage II corresponding to N supplies of 80 and 60%, respectively) boosted the accumulation of PHB in the cultivation broth (while maintaining a good system performance throughout the entire test only in stage II). Therefore, the volumetric PHB productivities (12 g-PHB m^{-3} d^{-1}) corresponding to the end of stage II in Test Series 2 increased by a factor of ~4 compared to continuous cultivation. These results evidenced the need of decoupling both growth and PHB synthesis phases to achieve improved PHB productivities. The assessment of the long-term operation under N feast-famine cycles of 8 h:16 h (stage II, Test Series 2) would be required as microbial stability might be affected in the long-term by the low dilution rate and the accumulation of dissolved metabolites such as formaldehyde (up to 120 mg-TOC L^{-1} were measured by the end of the stage II) (Marx et al., 2004). The 24 h:24 h feast-famine strategy (50% N supply – Test Series 3) featured PHB contents of 22% and the highest PHB productivity (20 g-PHB m^{-3} d^{-1}), almost doubling the PHB productivities achieved during shorter cycles (Test Series 2) with a stable methane elimination capacity. These productivities were comparatively lower than those reported for *M. hirsuta* (~50 g-PHB m^{-3} d^{-1}) by Rodríguez et al. (2020b), who operated a bubble column bioreactor under 24 h:24 h cycles with higher CH_4-ECs and alternating supply of NMS and NFMS. On the other hand, a further increase to 48 h of N limitation (33% N supply – Test Series 4) resulted in PHB-rich cells (35.5%) and similar volumetric PHB productivities (21 g-PHB m^{-3} d^{-1}). Unfortunately, the process collapsed following 3 cycles of 24 h:48 h nitrogen feast:famine operation. Previous works subjecting *Methylocystis hirsuta* to N-deprivation periods of 48 h under continuous supply of methane/biogas also entailed a deterioration of the microbial activity followed by an eventual system collapse (García-Pérez et al., 2018; Rodríguez et al., 2020b). These outcomes underlined the need for optimizing the period under nitrogen limitation to guarantee a sustained CH_4 abatement and a maximum PHB content.

The scaling-up of this process is currently under study in a pilot scale unit (9 m^3) located in a biogas production facility within the framework of the European project URBIOFIN. In this context, the nitrogen feeding strategy that led to the highest PHB productivities will be implemented in the following months for the continuous production of PHB. Among main drawbacks, the use of pure cultures entails a high risk of microbial contamination in the bioreactor. Nonetheless, the purity of the methanotrophic cultures can be well-preserved if growth and nutrient depriving conditions provided are somehow balanced. Otherwise, the presence of predators (i.e. protozoa) can ocurr. Regarding the bioreactor, the stirred tank bioreactor is the dominant vessel of choice in the biotechnology industry. In this regard, lower stirring velocities may be considered for the scaling-up, which would decrease the shear stress in the culture at the expense of lower CH_4 mass transfer rates.

5. Conclusions

This work constitutes the first study assessing strategies for a continuous biogas-based PHB production by *M. parvus*. The best operational strategies supporting an effective PHB production (12–20 g PHB m^{-3} d^{-1}) without compromising process stability were based on nitrogen feast-famine cycles of 8 h:16 h and 24 h:24 h (representing stoichiometric nitrogen inputs of 80 and 50%, respectively). Conversely, exposures to nitrogen-limiting periods 2-folds higher than the duration of the nitrogen feeding phase (6 h:18 h, 4 h:20 h and 24 h:48 h) entailed a deterioration in methanotrophic activity at nitrogen inputs ≤60%. Continuous N feeding did not facilitate an effective PHB production despite nitrogen limitation. These results evidence that a proper design of the feast-famine phases and mineral medium is crucial to sustain stable CH_4 utilization and PHB production, and ultimately to efficiently scale up the biorefinery process.

CRediT author statement

Yadira Rodríguez: Investigation, Formal analysis, Visualization, Writing - original draft. **Silvia García:** Investigation. **Rebeca Pérez:** Investigation. **Raquel Lebrero:** Funding acquisition, Supervision, Writing - review & editing. **Raúl Muñoz:** Conceptualization, Funding acquisition, Supervision, Writing - review & editing.

Declaration of competing interest

The authors declare that they have no known competing financial interests or personal relationships that could have appeared to influence the work reported in this paper.

Acknowledgements

Authors gratefully acknowledge the financial support by the Spanish Ministry of Science and Innovation under grant agreement no. BES-2016-077160 (CTM2015-70442-R project). The support from the EU-FEDER programme and the regional government of Castilla y León (UIC 3015, CLU 2017–09) is also acknowledged. Authors sincerely thank V. Pérez for providing practical help with the experimental setup.

Appendix A. Supplementary data

Supplementary data to this article can be found online at https://doi.org/10.1016/j.chemosphere.2022.134443.

References

AlSayed, A., Fergala, A., Eldyasti, A., 2018. Sustainable biogas mitigation and value-added resources recovery using methanotrophs integrated into wastewater

treatment plants. Rev. Environ. Sci. Biotechnol. 17 (2), 351–393. https://doi.org/10.1007/s11157-018-9464-3.
Asenjo, J.A., Suk, J.S., 1986. Microbial Conversion of Methane into poly-β-hydroxybutyrate (PHB): growth and intracellular product accumulation in a type II methanotroph. J. Ferment. Technol. 64 (4), 271–278. https://doi.org/10.1016/0385-6380(86)90118-4.
Blunt, W., Levin, D.B., Cicek, N., 2018. Bioreactor operating strategies for improved polyhydroxyalkanoate (PHA) productivity. Polymers 10 (11). https://doi.org/10.3390/polym10111197.
Bordel, S., Rodriguez, Y., Hakobyan, A., Rodriguez, E., Lebrero, R., Munoz, R., 2019a. Genome scale metabolic modeling reveals the metabolic potential of three Type II methanotrophs of the genus Methylocystis. Metab. Eng. 54, 191–199. https://doi.org/10.1016/j.ymben.2019.04.001.
Bordel, S., Rojas, A., Munoz, R., 2019b. Reconstruction of a genome scale metabolic model of the polyhydroxybutyrate producing methanotroph Methylocystis parvus OBBP. Microb. Cell Factories 18 (1), 104. https://doi.org/10.1186/s12934-019-1154-5.
Cai, Y., Zheng, Y., Bodelier, P.L.E., Conrad, R., Jia, Z., 2016. Conventional methanotrophs are responsible for atmospheric methane oxidation in paddy soils. Nat. Commun. 7 (1), 11728. https://doi.org/10.1038/ncomms11728.
Cantera, S., Bordel, S., Lebrero, R., Gancedo, J., García-Encina, P.A., Muñoz, R., 2019. Bio-conversion of methane into high profit margin compounds: an innovative, environmentally friendly and cost-effective platform for methane abatement. World J. Microbiol. Biotechnol. 35 (1), 16. https://doi.org/10.1007/s11274-018-2587-4.
Chen, X., Rodríguez, Y., López, J.C., Muñoz, R., Ni, B.J., Sin, G., 2020. Modeling of polyhydroxyalkanoate synthesis from biogas by Methylocystis hirsuta. ACS Sustain. Chem. Eng. 8 (9), 3906–3912. https://doi.org/10.1021/acssuschemeng.9b07414.
Choi, S.Y., Cho, I.J., Lee, Y., Kim, Y.J., Kim, K.J., Lee, S.Y., 2020. Microbial polyhydroxyalkanoates and nonnatural polyesters. Adv. Mater. 32 (35), 1907138. https://doi.org/10.1002/adma.201907138, 1-37.
del Cerro, C., García, J.M., Rojas, A., Tortajada, M., Ramón, D., Galán, B., Prieto, M.A., García, J.L., 2012. Genome sequence of the methanotrophic poly-β-hydroxybutyrate producer Methylocystis parvus OBBP. J. Bacteriol. 194 (20), 5709. https://doi.org/10.1128/jb.01346-12.
EBA, 2020. EBA Statistical Report. European Biogas Association. https://www.europeanbiogas.eu/wp-content/uploads/2021/01/EBA_StatisticalReport2020_abridged.pdf. (Accessed March 2021).
EuropeanBioplastics, novaInstitute, 2020. Bioplastics Market Data. https://www.european-bioplastics.org/market/. (Accessed May 2021).
García-Pérez, T., López, J.C., Passos, F., Lebrero, R., Revah, S., Muñoz, R., 2018. Simultaneous methane abatement and PHB production by Methylocystis hirsuta in a novel gas-recycling bubble column bioreactor. Chem. Eng. J. 334, 691–697. https://doi.org/10.1016/j.cej.2017.10.106.
Hanson, R.S., Hanson, T.E., 1996. Methanotrophic bacteria. Microbiol. Rev. 60 (2), 439–471. https://doi.org/10.1128/mr.60.2.439-471.1996.
Heidbreder, L.M., Bablok, I., Drews, S., Menzel, C., 2019. Tackling the plastic problem: a review on perceptions, behaviors, and interventions. Sci. Total Environ. 668, 1077–1093. https://doi.org/10.1016/j.scitotenv.2019.02.437.
Hoefman, S., van der Ha, D., Boon, N., Vandamme, P., De Vos, P., Heylen, K., 2014. Niche differentiation in nitrogen metabolism among methanotrophs within an operational taxonomic unit. BMC Microbiol. 14 (1), 83. https://doi.org/10.1186/1471-2180-14-83.
Jiang, G., Hill, D.J., Kowalczuk, M., Johnston, B., Adamus, G., Irorere, V., Radecka, I., 2016. Carbon sources for polyhydroxyalkanoates and an integrated biorefinery. Int. J. Mol. Sci. 17 (7) https://doi.org/10.3390/ijms17071157.
Karthikeyan, O.P., Chidambarampadmavathy, K., Cirés, S., Heimann, K., 2015. Review of sustainable methane mitigation and biopolymer production. Crit. Rev. Environ. Sci. Technol. 45 (15), 1579–1610. https://doi.org/10.1080/10643389.2014.966422.
Kaur, G., Roy, I., 2015. Strategies for large-scale production of polyhydroxyalkanoates. Chem. Biochem. Eng. Q. 29, 157–172. https://doi.org/10.15255/cabeq.2014.2255.
Khatami, K., Perez-Zabaleta, M., Owusu-Agyeman, I., Cetecioglu, Z., 2021. Waste to bioplastics: how close are we to sustainable polyhydroxyalkanoates production? Waste Manag. 119, 374–388. https://doi.org/10.1016/j.wasman.2020.10.008.
King, G.M., Schnell, S., 1994. Ammonium and nitrite inhibition of methane oxidation by methylobacter albus BG8 and Methylosinus trichosporium OB3b at low methane concentrations. Appl. Environ. Microbiol. 60 (10), 3508. https://doi.org/10.1128/aem.60.10.3508-3513.1994.
Koller, M., 2018. A review on established and emerging fermentation schemes for microbial production of polyhydroxyalkanoate (PHA) biopolyesters. Fermentatio 4 (2), 30. https://doi.org/10.3390/fermentation4020030.
Koller, M., Muhr, A., 2014. Continuous production mode as a viable process-engineering tool for efficient poly(hydroxyalkanoate) (PHA) bio-production. Chem. Biochem. Eng. Q. 28, 65–77.
Lebreton, L., Andrady, A., 2019. Future scenarios of global plastic waste generation and disposal. Palgrave Communications 5 (1), 6. https://doi.org/10.1057/s41599-018-0212-7.
Levett, I., Birkett, G., Davies, N., Bell, A., Langford, A., Laycock, B., Lant, P., Pratt, S., 2016. Techno-economic assessment of poly-3-hydroxybutyrate (PHB) production from methane - the case for thermophilic bioprocessing. J. Environ. Chem. Eng. 4, 3724–3733. https://doi.org/10.1016/j.jece.2016.07.033.
López, J.C., Arnáiz, E., Merchán, L., Lebrero, R., Muñoz, R., 2018. Biogas-based polyhydroxyalkanoates production by Methylocystis hirsuta: a step further in anaerobic digestion biorefineries. Chem. Eng. J. 333, 529–536. https://doi.org/10.1016/j.cej.2017.09.185.
López, J.C., Rodríguez, Y., Pérez, V., Lebrero, R., Muñoz, R., 2019. CH4-Based polyhydroxyalkanoate production: a step further towards a sustainable bioeconomy. In: Kalia, V.C. (Ed.), Biotechnological Applications of Polyhydroxyalkanoates. Springer Singapore, Singapore, pp. 283–321. https://doi.org/10.1007/978-981-13-3759-8_11.
Marx, C., Miller, J.A., Chistoserdova, L., Lidstrom, M.E., 2004. Multiple formaldehyde oxidation/detoxification pathways in burkholderia fungorum LB400. J. Bacteriol. 186 (7), 2173–2178. https://doi.org/10.1128/JB.186.7.2173–2178.2004.
Mühlemeier, I.M., Speight, R., Strong, P.J., 2018. Biogas, bioreactors and bacterial methane oxidation. In: Kalyuzhnaya, M.G., Xing, X.-H. (Eds.), Methane Biocatalysis: Paving the Way to Sustainability. Springer International Publishing, Cham, pp. 213–235. https://doi.org/10.1007/978-3-319-74866-5_14.
Muñoz, R., Meier, L., Diaz, I., Jeison, D., 2015. A review on the state-of-the-art of physical/chemical and biological technologies for biogas upgrading. Rev. Environ. Sci. Biotechnol. 14 (4), 727–759. https://doi.org/10.1007/s11157-015-9379-1.
Muñoz, R., Soto, C., Zuñiga, C., Revah, S., 2018. A systematic comparison of two empirical gas-liquid mass transfer determination methodologies to characterize methane biodegradation in stirred tank bioreactors. J. Environ. Manag. 217, 247–252. https://doi.org/10.1016/j.jenvman.2018.03.097.
Murrell, J.C., Dalton, H., 1983. Nitrogen-fixation in obligate methanotrophs. J. Gen. Microbiol. 129, 3481–3486. https://doi.org/10.1099/00221287-129-11-3481.
Myung, J., Flanagan, J.C.A., Waymouth, R.M., Criddle, C.S., 2017. Expanding the range of polyhydroxyalkanoates synthesized by methanotrophic bacteria through the utilization of omega-hydroxyalkanoate co-substrates. Amb. Express 7 (1), 118. https://doi.org/10.1186/s13568-017-0417-y.
Nyerges, G., Han, S.-K., Stein, L.Y., 2010. Effects of ammonium and nitrite on growth and competitive fitness of cultivated methanotrophic bacteria. Appl. Environ. Microbiol. 76 (16), 5648. https://doi.org/10.1128/AEM.00747-10.
Nyerges, G., Stein, L.Y., 2009. Ammonia cometabolism and product inhibition vary considerably among species of methanotrophic bacteria. FEMS Microbiol. Lett. 297 (1), 131–136. https://doi.org/10.1111/j.1574-6968.2009.01674.x.
Pérez, V., Lebrero, R., Muñoz, R., 2020. Comparative evaluation of biogas valorization into electricity/heat and poly(hydroxyalkanoates) in waste treatment plants: assessing the influence of local commodity prices and current biotechnological limitations. ACS Sustain. Chem. Eng. 8 (20), 7701–7709. https://doi.org/10.1021/acssuschemeng.0c01543.
Pieja, A.J., Sundstrom, E.R., Criddle, C.S., 2011. Poly-3-hydroxybutyrate metabolism in the type II methanotroph Methylocystis parvus OBBP. Appl. Environ. Microbiol. 77 (17), 6012–6019. https://doi.org/10.1128/AEM.00509-11.
Pieja, A.J., Sundstrom, E.R., Criddle, C.S., 2012. Cyclic, alternating methane and nitrogen limitation increases PHB production in a methanotrophic community. Bioresour. Technol. 107, 385–392. https://doi.org/10.1016/j.biortech.2011.12.044.
PlasticsEurope, 2020. Plastics - the Facts 2020. https://www.plasticseurope.org/en/resources/publications/4312-plastics-facts-2020. (Accessed May 2021).
Ramsay, B.A., Lomaliza, K., Chavarie, C., Dubé, B., Bataille, P., Ramsay, J.A., 1990. Production of poly-(beta-hydroxybutyric-co-beta-hydroxyvaleric) acids. Appl. Environ. Microbiol. 56 (7), 2093–2098. https://doi.org/10.1128/aem.56.7.2093-2098.1990.
Riedel, S.L., Brigham, C.J., 2020. Inexpensive and waste raw materials for PHA production. In: Koller, M. (Ed.), The Handbook of Polyhydroxyalkanoates: Microbial Biosynthesis and Feedstocks, first ed., vol. 1. CRC Press. https://doi.org/10.1201/9780429296611. first ed.
Rocha-Rios, J., Muñoz, R., Revah, S., 2010. Effect of silicone oil fraction and stirring rate on methane degradation in a stirred tank reactor. J. Chem. Technol. Biotechnol. 85 (3), 314–319. https://doi.org/10.1002/jctb.2339.
Rodríguez, Y., Firmino, P.I.M., Arnáiz, E., Lebrero, R., Muñoz, R., 2020a. Elucidating the influence of environmental factors on biogas-based polyhydroxybutyrate production by Methylocystis hirsuta CSC1. Sci. Total Environ. 706, 135136. https://doi.org/10.1016/j.scitotenv.2019.135136.
Rodríguez, Y., Firmino, P.I.M., Pérez, V., Lebrero, R., Muñoz, R., 2020b. Biogas valorization via continuous polyhydroxybutyrate production by Methylocystis hirsuta in a bubble column bioreactor. Waste Manag. 113, 395–403. https://doi.org/10.1016/j.wasman.2020.06.009.
Rostkowski, K.H., Pfluger, A.R., Criddle, C.S., 2013. Stoichiometry and kinetics of the PHB-producing Type II methanotrophs Methylosinus trichosporium OB3b and Methylocystis parvus OBBP. Bioresour. Technol. 132, 71–77. https://doi.org/10.1016/j.biortech.2012.12.129.
Sagong, H.-Y., Son, H.F., Choi, S.Y., Lee, S.Y., Kim, K.-J., 2018. Structural insights into polyhydroxyalkanoates biosynthesis. Trends Biochem. Sci. 43 (10), 790–805. https://doi.org/10.1016/j.tibs.2018.08.005.
Sipkema, E.M., de Koning, W., Ganzeveld, K.J., Janssen, D.B., Beenackers, A.A.C.M., 2000. NADH-regulated metabolic model for growth of Methylosinus trichosporium OB3b. Model presentation, parameter estimation, and model validation. Biotechnol. Prog. 16 (2), 176–188. https://doi.org/10.1021/bp9901567.
Steinbüchel, A., Valentin, H.E., 1995. Diversity of bacterial polyhydroxyalkanoic acids. FEMS (Fed. Eur. Microbiol. Soc.) Microbiol. Lett. 128 (3), 219–228. https://doi.org/10.1016/0378-1097(95)00125-O.
Sundstrom, E.R., Criddle, C.S., 2015. Optimization of methanotrophic growth and production of poly(3-hydroxybutyrate) in a high-throughput microbioreactor system. Appl. Environ. Microbiol. 81 (14), 4767. https://doi.org/10.1128/AEM.00025-15.
Trotsenko, Y.A., Murrell, J.C., 2008. Metabolic aspects of aerobic obligate methanotrophy. In: Advances in Applied Microbiology, vol. 63. Academic Press, pp. 183–229. https://doi.org/10.1016/S0065-2164(07)00005-6.
van den Oever, M., Molenveld, K., van der Zee, M., Bos, H., 2017. Bio-based and Biodegradable Plastics - Facts and Figures. Wageningen UR, p. 1722. https://doi.org/10.18174/408350.

Vandi, L.-J., Chan, C.M., Werker, A., Richardson, D., Laycock, B., Pratt, S., 2018. Wood-PHA composites: mapping opportunities. Polymers 10 (7). https://doi.org/10.3390/polym10070751.

Vecherskaya, M., Dijkema, C., Saad, H.R., Stams, A.J.M., 2009. Microaerobic and anaerobic metabolism of a Methylocystis parvus strain isolated from a denitrifying bioreactor. Environmental Microbiology Reports 1 (5), 442–449. https://doi.org/10.1111/j.1758-2229.2009.00069.x.

Whittenbury, R., Phillips, K.C., Wilkinson, J.F., 1970. Enrichment, isolation and some properties of methane-utilizing bacteria. Microbiology 61 (2), 205–218. https://doi.org/10.1099/00221287-61-2-205.